

Single Dye Molecule Fluorescence in Liquid Crystal Hosts

Nadine Lippa

Single Dye Molecule Fluorescence in Liquid Crystal Hosts

Nadine Lippa

BYRON-BERGEN HIGH SCHOOL
6717 West Bergen Rd.
Bergen, NY 14416

Advisors: Dr. Ansgar W. Schmid^{*)} and Dr. Svetlana G. Lukishova^{**)}

^{*)} LABORATORY FOR LASER ENERGETICS
University of Rochester
250 East River Road
Rochester, NY 14625-1299

^{**)} THE INSTITUTE OF OPTICS
University of Rochester
Rochester, NY 14627-0186

ABSTRACT

We have investigated single dye molecules embedded in liquid crystal hosts and created one prototype of an efficient room-temperature, deterministically polarized *single photon source* (SPS) *on demand* with nonclassical photon statistics (antibunching). SPS is a key hardware element in quantum information technology. Its use permits both secure communication systems based on the laws of quantum mechanics as well as extremely powerful quantum computers. We used planar-aligned *chiral* nematic (cholesteric) liquid crystal hosts for fluorescent dyes to take advantage of (1) deterministically polarized photons, and (2) excitation and fluorescence efficiency increases. We prepared 1-D photonic band gap cholesteric liquid crystal structures (both low molecular weight and Wacker oligomeric liquid crystals) doped with terrylene/rhodamine B dye molecules at exceedingly low concentration. We then performed a 532-nm, laser-induced confocal

fluorescence microscopy of the individual dye molecules in the liquid crystal hosts and measured fluorescence-photon statistics from liquid-crystal-embedded chromophores.

INTRODUCTION

The application of the project is an efficient, deterministically polarized single photon source on demand [1-3]. Single photon source (SPS) is a key hardware element for quantum information technology [4-7].

In order to produce single photons, it is necessary to excite a *single* emitter, for instance, a single dye molecule. That is why a laser beam should be tightly focused into a sample area containing a very low concentration of molecules, so that only one molecule becomes excited (Figure 1). It emits only one photon at a time: when this molecule is excited, it will remain in the excited state for a specific lifetime before emitting its own photon. Because of the lifetime, there will always be a pause between emissions of any two sequential photons. If one measures the number of second photons (coincidence events) that appear after each first photon at a definite time interval τ , the histogram should diminish to zero ordinate at $\tau = 0$ (see Figure 2). No two photons appear together at the same time. This is a manifestation of nonclassical photon statistics called *antibunching* [8-10].



Figure 1. Excitation of one emitter by the laser beam.

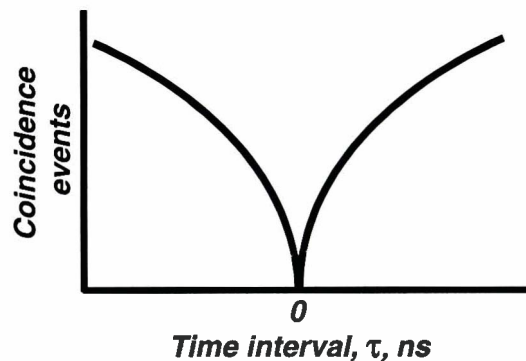


Figure 2. Explanation of antibunching.

The graph is *symmetric* relative to $\tau = 0$, because photons emitted are not labeled “first” or “second” in the emission process but become so only through the measurement. It does not matter whether a specific photon is “first” or “second”. What matters is the *delay in arrival times* (time interval) of any pair of photons .

In quantum information technology SPSs are used both for quantum cryptography (quantum communication) [4, 11-15] and for quantum computation [4-6]. In quantum communication, using SPS prevents an eavesdropper from being allowed to intercept, without the sender/receiver’s knowledge, a message with secret encryption key (Figure 3). Any e-mail message, telephone call, credit card information and other financial transaction will be safe. They will be protected by the Heisenberg uncertainty principle: if you try to measure the behavior of a quantum particle, you alter it in such a way that your measurement isn’t completely accurate. This means if you send the encryption key using *single photons*, no one can steal them without your knowledge.

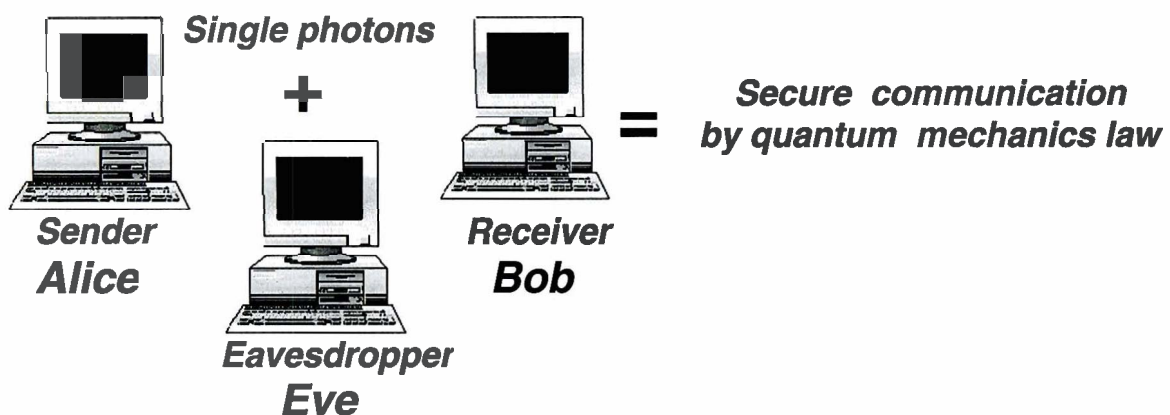


Figure 3. Quantum cryptography schematic.

Modern quantum cryptography systems are using laser pulses highly attenuated down to the single-photon level [13]. For instance, such a highly attenuated laser source is currently being applied to a cryptography system using a 67-km long, Swisscom telecommunication fiber link under Lake Geneva in Switzerland [13, 15]. However, the lack in efficiency is evident. Nine out of ten attempts to fire a photon fail with such weak laser pulses [13]. Efficient SPS realization that provides polarized single photons on demand with each pulse and with a high repetition rate is pivotal for practical quantum cryptography. In another implementation, SPS becomes the key hardware element for extremely powerful quantum computers with linear optical elements and photodetectors [16,17].

A range of solutions for SPSs is presented in the literature. SPSs have recently been demonstrated, using a variety of devices, including single molecules, single color centers in diamond, single trapped ions, and various semiconductor quantum dots, see reviews [18-20]. However, there remain significant disadvantages that hinder the establishment of a commercial product. Most SPSs, based on semiconductor heterostructures, operate at liquid helium temperature [21]. The SPS solutions that operate at room temperature, besides single dye molecule fluorescence, have emitters with long fluorescence lifetimes and they are not polarized deterministically. For instance, the single-nitrogen-vacancy (NV) center in diamond [22] has 11.6-ns lifetime in monocrystals and 23 ns in polycrystals. Dye molecules have much shorter fluorescence lifetimes, e.g., terrylene dye molecules provide a fluorescence lifetime of ~3.2-ns, preferred for high-data-rate transmission. It should be noted that single photons from most known SPSs are not polarized deterministically. It is very important for

quantum cryptography protocols and for quantum logic operations to have a deterministic polarization state of single photons.

The purpose of this study is to provide a way for an efficient, room temperature single photon source on demand with *deterministically polarized* photons. To reach this goal, liquid-crystal hosts' advantages are used to modify the properties of single-dye-molecule fluorescence. First of all, liquid-crystal technology permits one to align the nematic liquid crystal host and the embedded dye molecules in a direction preferable for maximum excitation efficiency of the dye dipole with the excitation-field electric field vector parallel to the molecular alignment axis. Deterministically aligned dye molecules will also provide deterministically polarized emission photons. In addition, 1-D photonic bandgap chiral nematic (cholesteric) liquid-crystal structures will provide up to one order of magnitude efficiency increase of the SPS [19] in comparison with other SPSs based on single-dye-molecule fluorescence [23].

This paper consists of two main parts:

- (1) material science and technology,
- (2) optical radiation science.

The material science and technology part describes planar-aligned liquid-crystal-sample preparation and doping with dye at extremely low concentration. In particular, the preparation and investigation of selective reflection properties of 1-D photonic bandgap structures in cholesteric liquid crystals will be discussed. The second, optical-radiation-science part comprises description of confocal fluorescence microscopy of single dye molecules in liquid crystal hosts and photon statistics measurements to look for antibunching.

1. MATERIAL SCIENCE PART:

PREPARATION OF 1-D PHOTONIC BANDGAP CHOLESTERIC LIQUID CRYSTAL STRUCTURES DOPED WITH SINGLE DYE MOLECULES

A photonic bandgap material is a periodic structure that totally reflects light of a certain wavelength range, prohibiting its propagation through the structure [24]. To create a photonic bandgap structure in cholesteric liquid crystal, planar alignment of cholesteric liquid crystal at the device boundaries, i.e., cell substrates, assists the self-assembly.

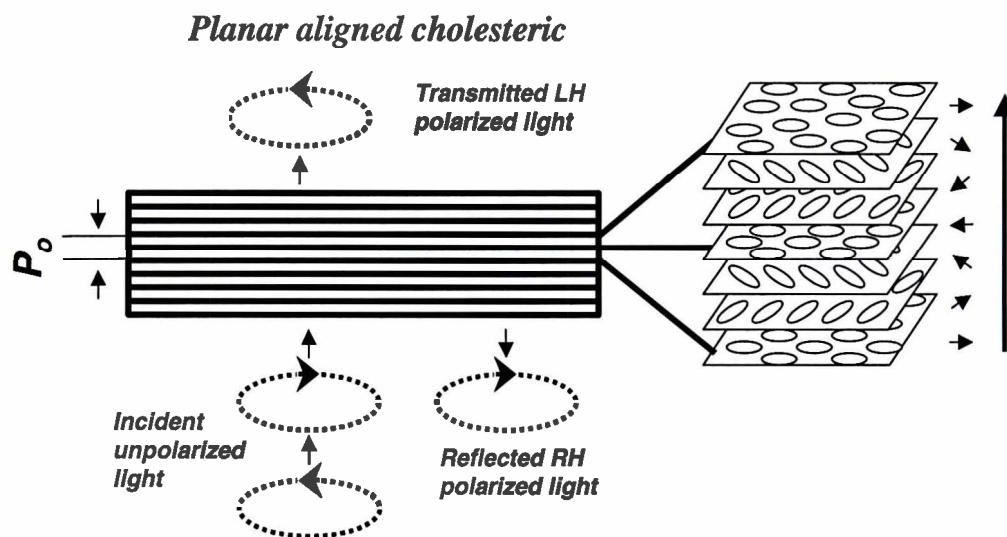


Figure 4. Cholesteric liquid crystal 1-D photonic bandgap structure schematics.

In *planar* aligned cholesterics, that for visualization purposes can be described as consisting of a periodically layered structure, the axes of the molecular director (rightmost set of arrows in Figure 4) rotate monotonically to form a periodic helical structure with pitch P_0 [25]. For such a liquid-crystal structure, the reflectance of normally incident, circularly polarized light with electric-field vector-rotation opposite to

the rotation of molecules in the helical structure (Bragg condition), approaches 100% within a band centered at

$$\lambda_0 = n_{av}P_0, \quad (1)$$

where $n_{av} = (n_e + n_o)/2$ is the average of the ordinary and extraordinary refractive indices of the medium. This is the so-called selective reflection of cholesteric liquid crystals. The bandwidth is

$$\Delta\lambda = \lambda_0\Delta n/n_{av}, \quad (2)$$

where $\Delta n = n_e - n_o$. Such a periodic structure can also be viewed as a 1-dimensional photonic crystal, with a bandgap within which propagation of light at λ_0 is forbidden. For emitters located within such a structure, the rate of spontaneous emission is suppressed within the spectral stop band and enhanced near the band edge [26]. It is this enhancement that helps the performance improvement in current SPSs.

1.1. Substrate and sample preparation for single molecule fluorescence microscopy and planar alignment of liquid crystals

Single-molecule fluorescence microscopy imposes two requirements on the samples: (1) no fluorescent *impurities* should be left on the substrates; (2) 180 and 300 μm -working distance of high N.A. objectives permits use only of samples with thickness not exceeding this value. For this reason, $\sim 170\text{-}\mu\text{m}$ -thickness glass microscopic cover slip substrates were used that both are fragile and need special care in handling. Liquid-crystal cells were fabricated in a class 1,000 liquid-crystal clean-room facility of the Optical Materials Laboratory at LLE. Ultrasonic cleaning for 60 minutes freed the 1" x 1" substrates from any dirt particles. Substrates were then rinsed in flowing, deionized

water, and dried in a stream of compressed nitrogen. After that, they were etched in piranha solution ($\text{H}_2\text{SO}_2 + \text{H}_2\text{O}_2$ in equal volume concentration) for about 20 minutes, rinsed in flowing, deionized water and dried in a stream of oil-free nitrogen (liquid-nitrogen tank boil-off).

To prepare the 1-D photonic bandgap structures, three different planar alignment procedures for liquid crystals were used: (i) substrate shearing, (ii) buffing, and (iii) photoalignment. For sheared samples, no additional substrate coatings were needed. For buffing, substrates were spin coated with either of two polymers: Nylon-6 or Polyimide. For buffing, we used a standard, velvet-surface buffing machine (see Figure 5, left). To prevent damage to the fragile substrates during the buffing procedure, cover slips were “blocked to” 1-mm-thick microscope slides with water-soluble acetate, using 40-min heating at 80°C for better results. After buffing, the cover slips were unblocked in standing, deionized water over night. This was followed by a rinse in flowing, deionized water to rid the samples of acetate traces. For photoalignment, substrates were spin-coated with Staralign 2100 from Vantico Inc. Photoalignment of coated polymer was achieved using six, UV discharge lamps with maximum wavelength ~ 302 nm (40 nm bandwidth) and a UV linear dichroic polarizer placed in a hermetic box (see Figure 5, right). The photoalignment procedure at ~ 5 mW/cm^2 power density at 302 nm lasted 10 minutes.

We used two types of liquid crystals: Wacker oligomer cholesteric-liquid-crystal powders, and low-molecular-weight E7 + CB15 (chiral additive) monomeric mixtures. For the Wacker oligomer liquid crystal powders, the samples were prepared by mixing different concentrations of two powders with individually known selective-reflection

wavelengths (vendor information). In order to obtain a desired selective-reflection wavelength mixture, mixing rules were empirically found from a set of multiple, different mixtures. To change the pitch of each mixture, powders were dissolved in methanol, mixed for 2 hours under agitation and at elevated temperature, purified through 0.45- μm particle filters, and dried from solvent under vacuum. For planar alignment, an uncoated, cleaned cover slip with a Wacker powder was placed on a hot plate and melted at 118°C. A second cover slip was used to shear the melted oligomer at temperature (and to also form the second window of the liquid-crystal cell). Slowly cooling the cell to room temperature froze in the planar alignment. For some Wacker powders, we used spin coating with polyimid and buffing of substrates. Cells with known and uniform thickness (10 –15 μm) were created by using 4 drops of a UV-cured epoxy mixed with calibrated, glass-bead spacers at the substrates' corners. After that, cells containing Wacker powder were heated into the isotropic phase and slowly cooled.

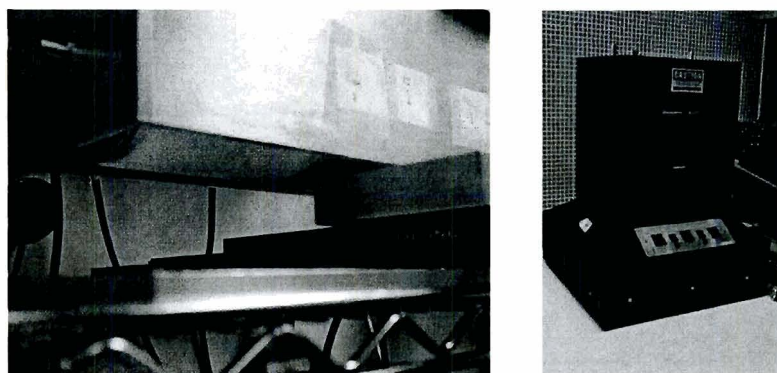


Figure 5. Buffing machine (left) and photoalignment apparatus. (right).

For low-molecular-weight liquid crystals, the coated substrate surfaces were either buffed or photoaligned. Cell thickness was again set by UV-epoxy mixed with glass-bead spacers. To find the weight concentration of the components C in a mixture of

chiral additive and nematic liquid crystal with desired selective reflection wavelength λ_0 we used a well-known relationship

$$C = n_{av}/(\lambda_0 \text{ HTP}), \quad (3)$$

where HTP is the *helical twisting power* of the chiral additive in a nematic liquid crystal. For CB15 in E7, $\text{HTP} \approx 7.3\mu\text{m}^{-1}$. An E7+CB15 liquid crystal mixture with selected concentration was fed through a 0.45- μm particle filter and a stainless-steel syringe into the assembled cell *parallel* to the polymer-alignment direction encribed in the cell walls.

Typical, prepared samples with 1-D photonic-bandgap liquid-crystal structures (both Wacker oligomers and CB15 + E7 mixtures) are depicted in Figure 6.

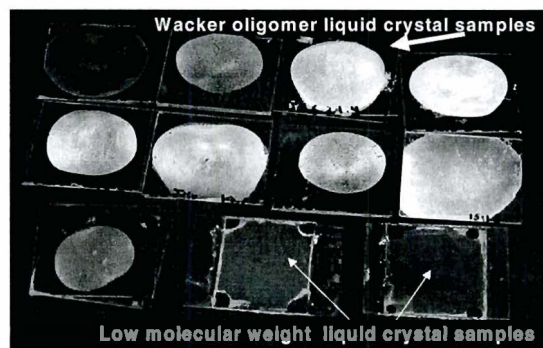


Figure 6. Prepared 1-D photonic bandgap cholesteric liquid crystal cells.

Dye dopants used were, most commonly, *terrylene*, but also *rhodamine B*. We used *terrylene* solution in methylene chloride and *rhodamine B* solution at 10^{-8} M concentration in methanol. Optimized *terrylene* concentration was found empirically by stepwise diluting the starting solution, spin coating each time a cleaned but unaligned substrate, and testing each substrate for presence of predominant single-photon-emission behavior. The final *terrylene* solution was mixed with an equal amount of liquid crystal (by volume) and dried under vacuum.

1.2. Measurements of selective reflection of the 1-D photonic bandgap cholesteric liquid crystal samples in circularly polarized light

We used a Perkin Elmer *Lambda 900* spectrophotometer to measure the wavelength response of each prepared sample, thereby determining the specific selective reflection (photonic bandgap) for each sample. A zero-order quarter wave plate and a thin-film linear polarizer were used in both spectrophotometer channels to create circularly polarized incident light of the desired handedness. Samples were tested in unpolarized, as well as in left-handed and right-handed circularly polarized incident light. Figure 7 shows transmittance of Wacker oligomer cholesteric-liquid-crystal samples versus wavelength in left-handed circularly polarized light. Two mixtures (dotted lines) exhibit a bandgap edge around 579 nm, the fluorescence maximum of terrylene dye (vertical dotted line).

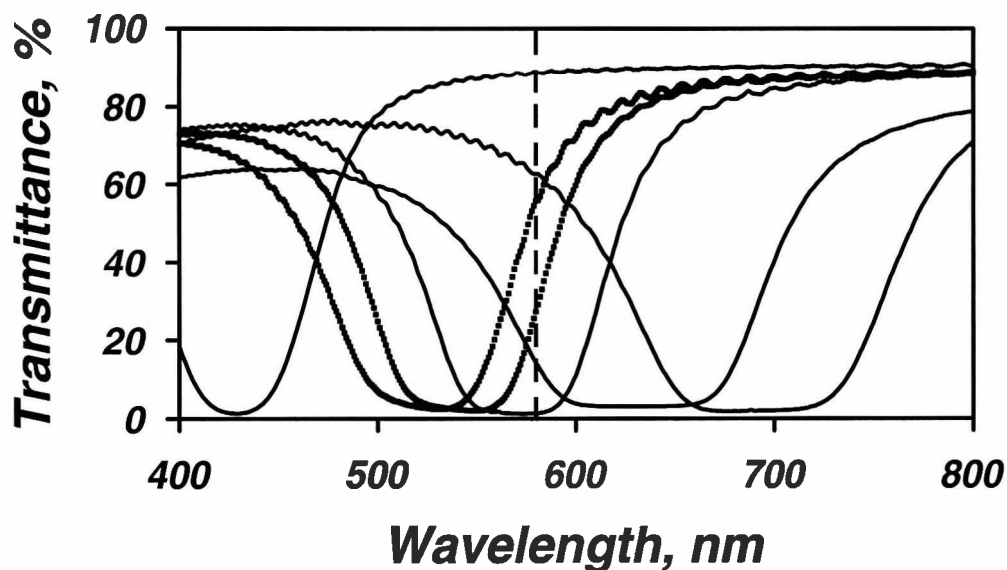


Figure 7. Transmittance curves of different Wacker oligomer 1-D photonic bandgap cholesteric liquid crystal structures. Planar alignment was made with substrates' shearing.

Similar results were achieved with the E7 + CB15 mixtures, both with buffed polyimid/nylon (Figure 8) and with photoalignment (Figure 9), in right-handed circularly polarized light (handedness strictly determined by the CB15 structure).

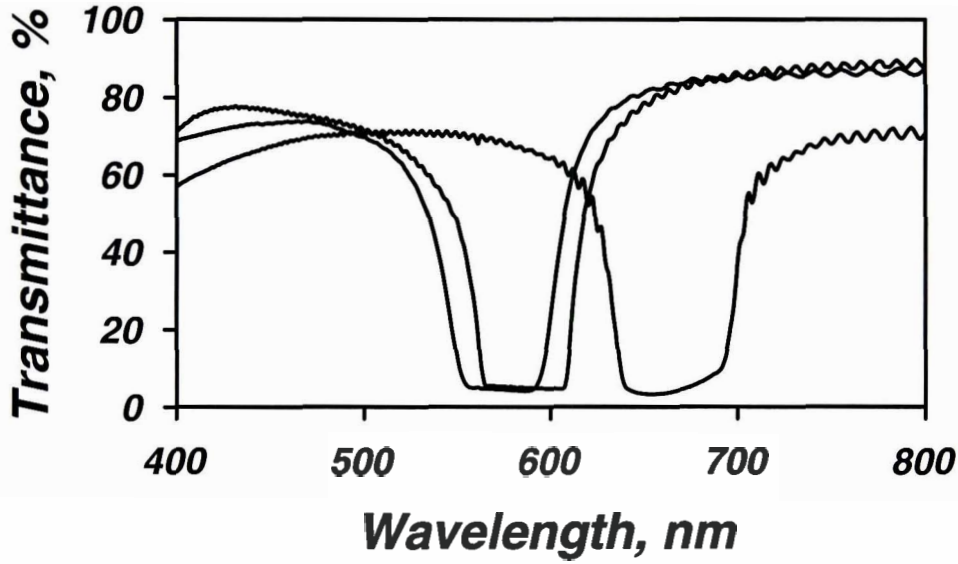


Figure 8. Transmittance curves of different E7 + CB15 mixture 1-D photonic bandgap cholesteric liquid crystal structures. Planar alignment was made with substrates' buffing.

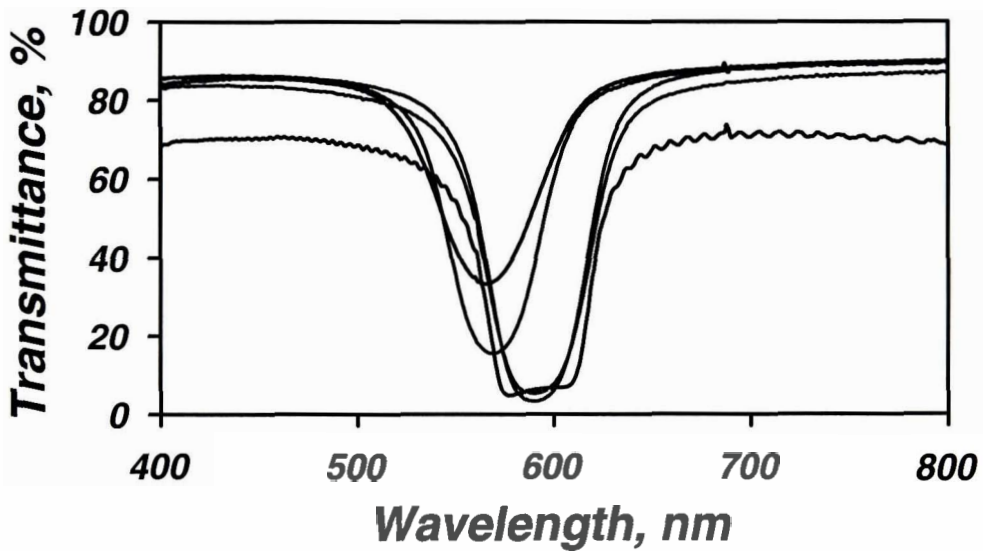


Figure 9. Transmittance curves of different E7+CB15 mixture 1-D photonic bandgap cholesteric liquid crystal structures. Planar alignment was made with photoalignment.

2. OPTICAL RADIATION SCIENCE PART: SINGLE-DYE MOLECULE FLUORESCENCE MICROSCOPY AND PHOTON STATISTICS MEASUREMENTS

2.1. Experimental setup

The experimental setup to test whether or not emission from a single emitter took place is shown in Figure 10. A 532-nm CW laser was focused by the 60x, 0.8 N. A. objective of an Alpha-SNOM confocal microscope of Witec (Figure 11) onto each doped sample. A second 100x, 1.4 N.A. infinity-corrected objective collected transmitted and emitted light contributions. Two interference filters rejected the laser light at 532-nm. A 25 μm /125 μm diameter (core/cladding) optical fiber formed the confocal aperture, and transported the light to a fiber 50:50, nonpolarizing beamsplitter of a Hanbury Brown and Twiss correlation setup [27]. Two avalanche photodiodes (Perkin Elmer SPCM-14 modules) registered the photons.

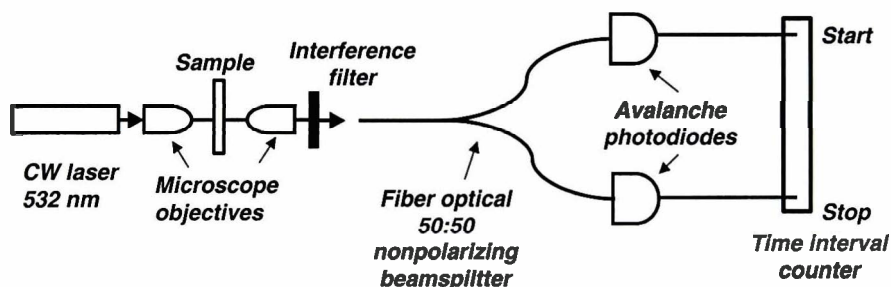


Figure 10. Experimental setup schematics for single-molecule fluorescence microscopy and photon statistics measurements.

For photon statistics measurements (see Chapter 2.3 for details), a CAMAC-based time to digital converter (Philips Scientific model 7186) controlled through the Internet or a time interval counter (Stanford Research Systems model SR620) with a pulse generator

and an oscilloscope (see Figure 12) were used to collect histograms of coincidence events.

For the purpose of observing more than one sample focal volume ($\sim 0.5 \mu\text{m}$ diameter laser beam, diffraction limit), the microscope offered a piezo-controlled stage that enabled raster scanning in the x-y directions for up to $100 \mu\text{m} \times 100 \mu\text{m}$ range. Ultimately there were two tests for single-emitter presence: (i) scanned images showing single-molecule blinking and bleaching events as well as (ii) antibunching histograms.

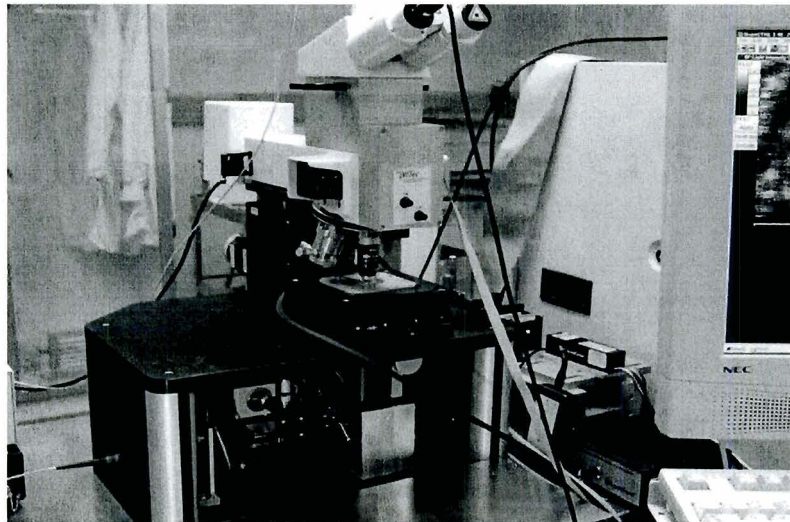


Figure 11. Photograph of the Alpha SNOM microscope.

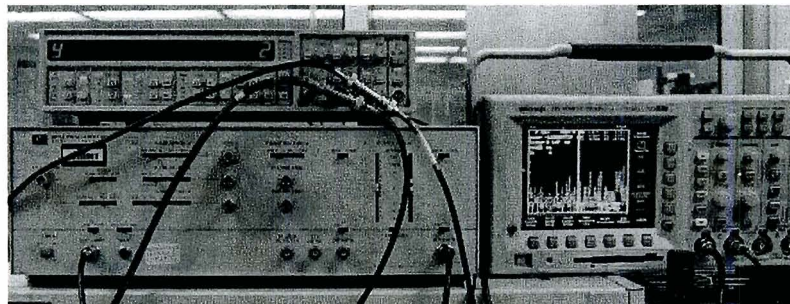


Figure 12. Equipment for photon statistics measurements: the time interval counter (top left corner) with the pulse generator (bottom left corner) and the oscilloscope with a histogram on the screen.

2.2. Experimental results on confocal fluorescence microscopy of single dye molecules

Typical fluorescence scans had dimensions of $10\ \mu\text{m} \times 10\ \mu\text{m}$, but sometimes ranged from $5\ \mu\text{m}$ to $30\ \mu\text{m}$, generally of 512×512 pixel resolution. Times taken for each of the 512 scanning lines were usually between 2.0 s and 8.0 s, producing images of varying contrast.

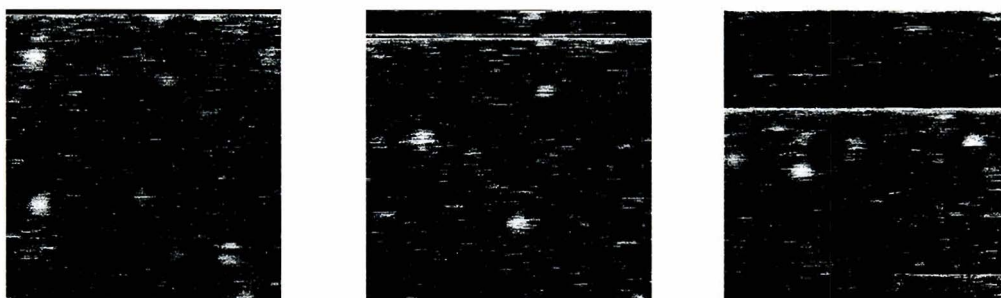


Figure 13. Confocal fluorescence microscopy images of single terrylene molecules ($10\ \mu\text{m} \times 10\ \mu\text{m}$ scans).

The results of confocal fluorescence microscopy of single dye molecules are visible in the images of Figure 13 obtained from Alpha SNOM. Single dye molecules are visible and show characteristic phenomena: “bleaching” and “blinking.” At the employed excitation power densities of $\sim 5\ \text{kW}/\text{cm}^2$, the finite probability for molecular dissociation in the intense photon field becomes experimentally observable. As the scan progresses, a certain number of molecules will suddenly cease emitting without ever recovering. This is generally referred to as “bleaching” (photolytic dissociation). Since no two emitters will dissociate at exactly the same moment, the observation of bleaching is accepted proof that whatever bleached was indeed a single molecule only. In addition, it was essential to assign the actual scan area a safe distance away from the laser $x = 0, y = 0$ parking position, because, with the laser at rest, massive, accumulative bleaching quickly

occurs during setup prior to the scan. “Blinking” is also evident in Figure 13. There are single lines within the molecule image that are not lit, showing that the fluorescence stopped for some time periods and later resumed, a phenomenon widely accepted as proof for the presence of single molecule fluorescence. Any two or more uncorrelated emitters would, at room temperature, not blink exactly in phase. The period of visible blinking ranges from several ms to several seconds. The detailed explanation of this long-time blinking remains controversial and subject to debate in the current literature [28].

2.3. Photon statistics measurements

Photon statistics measurements were taken with the time-to-digital converter or with the time interval counter. They detect the time interval τ between any “start” photon, which is detected by the first avalanche photodiode, and a “stop” photon, detected by the second avalanche photodiode. The time interval counter is attached to an oscilloscope for graphical presentation of the output data in a form of histogram of coincidence events versus τ . Photon statistics is defined from this histogram (Figure 14). The total number of events for time interval 1s is 10^6 , time resolution is 25 ps.

The photon-statistics measurements varied. In the group’s previous samples, antibunching was evident. In Figure 14 an absence of antibunching is encountered in recent samples, two reasons for this tend to dominate. The first is simply an overabundance of emitters, such that no single emitter is found alone, i.e., the dye concentration is still too high. Another potential contributor to polluted emission is background from impurities that the substrate-buffing process deposited. At 10 – 15 μm cell thickness, the fluorescence contributions from the substrate interfaces cannot be

completely eliminated by the confocal imaging approach. In addition, not all samples were tested yet. Because of the large amount of samples it is necessary to pursue this experiment further to attain more accurate and reliable results.

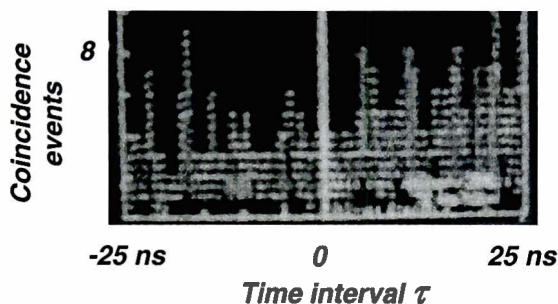


Figure 14. The photon statistics histogram of terrylene fluorescence from one of the prepared samples.

3. CONCLUSION AND FUTURE STEPS

Taken together, these results demonstrate that the cholesteric liquid-crystal system in conjunction with terrylene dopant constitutes a suitable and very promising room-temperature, single photon source. What needs to be further demonstrated, however, is the issue of high reliability emission *on demand*. This will require replacing the CW laser source used throughout this effort with a short-pulse excitation laser. Only under such excitation will it become clear whether or not single dye molecules exceed in performance the Swisscom source by emitting one and one photon only *for each excitation pulse*.

4. ACKNOWLEDGEMENTS

The author acknowledges Dr. A. Schmid and Dr. S. Lukishova for advising the project, and Dr. S. Craxton for organizing the research program. The author thanks also the Optical Materials Laboratory personnel at the LLE, especially K. Marshall and J.

Starowitz for their support and help, C. Supranowitz for the help, Prof. S. Chen's Laboratory for the loan of waveplates, and D.A. Voloschenko for consultation. Receipt of oligomer cholesteric liquid crystal powders starting material from Dr. F. Kreuzer of Wacker, Munich is also acknowledged.

Special thanks for the financial support of LLE for the summer program. The whole SPS project is supported by the U.S. Army Research Office under Award No. DAAD19-02-1-0285. Some equipment used is by the support of the U.S. Department of Energy Office of Inertial Confinement Fusion under Cooperative Agreement No. DE-FC03-92SF19460, the University of Rochester, and the New York State Energy Research and Development Authority. The support of DOE does not constitute an endorsement by DOE of the views expressed in this presentation.

REFERENCES

1. Solid state sources for single photons, www.iota.u-psud.fr/~S4P/.
2. P. Jonsson, "Generation, detection and applications of single photons", *Doctoral Dissertation*, Stockholm, Royal Inst. of Technology, 101 pp. (2002).
3. S. Benjamin, "Single photons "on demand"", *Science*, **290**, 2273-2274 (2000).
4. M. A. Nielsen and I. L. Chuang, *Quantum computation and quantum information*, Cambridge: Cambridge Univ. Press, 676 pp. (2001).
5. D. Bouwmeester, A. Ekert, A. Zeilinger, Eds., *The physics of quantum information: quantum cryptography, quantum teleportation, quantum computation*, Springer: Berlin, 314 pp. (2000).
6. The Center for Quantum Computation *Web site* (Oxford): www.qubit.org.
7. M.A. Nielsen, "Rules for a complex quantum world", *Scient. Amer.*, 67-75, Nov. (2002).

8. H.J. Kimble, M. Dagenais, L. Mandel, "Photon antibunching in resonance fluorescence", *Phys. Rev. Lett.*, **39**, 691-695 (1977).
9. D.F. Walls and G.J. Milburn, *Quantum Optics*, p.42, Springer-Verl., Berlin-NY, 351 pp. (1995).
10. U. Mets, "Antibunching and rotational diffusion in FCS", 346-359, in R. Rigler and E.S. Elson, Eds., *Fluorescence correlation spectroscopy. Theory and applications*, Springer, Berlin-NY (2001).
11. N. Gisin, G. Ribordy, W. Tittel, and H. Zbinden, "Quantum cryptography", *Rev. Mod. Phys.*, **74**, 145-195 (2002).
12. W.P. Risk and D.S. Bethune, "Quantum cryptography", *Opt. & Phot. News*, 26, July (2002).
13. A. Hart-Davis, "Can you keep a secret?" *Nature*, **418**, 270-272 (2002).
14. Company *MagiQ Technologies*, see <http://www.magiqtech.com>
15. Company *id Quantique*, see <http://www.idquantique.com>
16. E. Knill, R. Laflamme, and G.J. Milburn, "A scheme for efficient quantum computation with linear optics", *Nature*, **409**, 46-52 (2001).
17. A. Shields, "Quantum logic with light, glass and mirrors", *Science*, **297**, 1821-1822 (2002).
18. S.G. Lukishova, A.W. Schmid, A.J. McNamara, R.W. Boyd, and C. Stroud, Jr., "Demonstration of a room-temperature single-photon source for quantum information: single-dye-molecule fluorescence in a cholesteric liquid crystal host", *LLE Review*, Quarterly Report, **94**, 97-106, DOE/SF/19460-485, January – March (2003).
19. S.G. Lukishova, A.W. Schmid, A.J. McNamara, R.W. Boyd, and C. Stroud, Jr., "Room temperature single photon source: single dye molecule fluorescence in liquid crystal host", *IEEE J. Selected Topics in Quantum Electronics*, Special Issue on Quantum Internet Technologies, Nov-Dec. (2003), accepted for publication.

20. S.G. Lukishova, A.W. Schmid, C.M. Supranowitz, N. Lippa, A.J. McNamara, R.W. Boyd, and C.R. Stroud Jr., *J. Modern Optics*, Special issue on Single Photons, accepted for publication.
21. C. Santori, Fattal, D., Vuckovic, J., Solomon, G. & Yamamoto, Y. "Indistinguishable photons from a single-photon source," *Nature*, **419**, 594-597 (2002).
22. C. Kurtsiefer, S. Mayer, P. Zarda, H. Weinfurter, "Stable solid-state source of single photons", *Phys. Rev. Lett.*, **85**, 290-293 (2000).
23. B. Lounis and W.E. Moerner, "Single photons on demand from a single molecules at room temperature", *Nature*, **407**, 491-493 (2000).
24. E. Yablonovitch, "Inhibited spontaneous emission in solid-state physics and electronics", *Phys. Rev. Lett.*, **58**, 2059-2062 (1987).
25. S. Chandrasekhar, *Liquid Crystals*, Cambridge: Cambridge Univ. Press (1977).
26. V.P. Kopp, B. Fan, H.K.M. Vithana and A.Z. Genack, "Low threshold lasing at the edge of a photonic stop band in cholesteric liquid crystals", *Opt. Lett.*, **23**, 1707-1709 (1998).
27. R. Hanbury Brown, R.Q. Twiss, "Correlation between photons in two coherent beams of light, *Nature*, **177**, 27-29 (1956).
28. F. Vargas, O. Hollricher, O. Marti, G. de Schaetzen, G. Tarrach, "Influence of protective layers on the blinking of fluorescent single-molecules observed by confocal microscopy and scanning near field optical microscopy", *J. Chem. Phys.*, **117**, 866-871 (2002).